Interface energy analysis of III–V islands on Si (001) in the Volmer-Weber growth mode

Anne Ponchet, G. Patriarche, J. B. Rodriguez, L. Cerutti, E. Tournié

Interface energy analysis of III–V islands on Si (001) in the Volmer-Weber growth mode

Cite as: Appl. Phys. Lett. **113**, 191601 (2018); https://doi.org/10.1063/1.5055056
Submitted: 06 September 2018 • Accepted: 17 October 2018 • Published Online: 05 November 2018

A. Ponchet, G. Patriarche, J. B. Rodriguez, et al.

Interface energy analysis of III–V islands on Si (001) in the Volmer-Weber growth mode

A. Ponchet,[1,a)] G. Patriarche,[2] J. B. Rodriguez,[3] L. Cerutti,[3] and E. Tournié[3]
[1]*CEMES-CNRS, Université de Toulouse, UPS, 31055 Toulouse, Cedex 04, France*
[2]*Centre de Nanosciences et de Nanotechnologies, CNRS, Université Paris Sud, Université Paris Saclay, Avenue de la Vauve, 91120 Palaiseau, France*
[3]*IES, University Montpellier, CNRS, 34095 Montpellier, Cedex 5, France*

(Received 6 September 2018; accepted 17 October 2018; published online 5 November 2018)

The experimental island shapes of III–V islands grown on silicon (001) in the Volmer-Weber growth mode are analyzed in the frame of the theory of wetting in crystals. A reverse Wulff-Kaishew (or Winterbottom) construction is used in order to access interfacial energy. We apply this approach to AlSb and GaSb islands on (001) Si grown by molecular beam epitaxy and observed by scanning transmission electron microscopy. Experimental ratios between energies of (001), (110), (111)A, and (111)B surfaces are established. Interface energies are then quantitatively estimated for GaSb/Si and AlSb/Si interfaces. The differences in the shape of GaSb and AlSb islands, which are consistently reported in the literature, can be clearly attributed to a higher energy for the GaSb/Si interface compared to the ASb/Si one and not to different adatom diffusion lengths. The difference in interface energies is quantified, and its origin at the microscopic level is discussed. *Published by AIP Publishing.* https://doi.org/10.1063/1.5055056

Integration of III–V photonics and electronics on silicon should benefit from both III–Vs and Si worlds.[1,2] The emergence of viable devices however requires high crystal quality layers. Still, a number of issues have been identified with the epitaxy of III–Vs on (001) Si:[3] the 3D Volmer-Weber (VW) growth mode, the plastic relaxation, the stacking faults and twins in individual islands, and the antiphase boundaries formed when neighboring islands with different polarity orientations coalesce. Although the VW growth mode of III–Vs on Si was recognized early, the growth process driven by the wetting mechanisms was generally not investigated and thus not described in a theoretical frame.

Here, we focus on group III antimonides grown by molecular beam epitaxy (MBE) as a case study material. GaSb islands grown on (001) Si are very high relative to their width, sometimes even polycrystalline, and exhibit {001}, {111}, and {110} facets.[4–6] GaSb thick layers are consequently highly defective and not suitable for applications. In a precursor work, Akahane *et al.*[4] grew first a thin AlSb layer on the Si substrate to form a template. Thereafter, GaSb layers of much better quality than on bare Si were grown on AlSb/Si templates.[4–7] AlSb islands (or GaSb islands on AlSb/Si templates) are flatter than GaSb ones.[4–6] When seen in top view, they are also elongated,[4] while GaSb islands appeared rounded or isotropic.[4,5] These shape differences, consistently observed, were attributed to a shorter diffusion length of Al than Ga on the Si surface. In addition, in spite of a 14% misfit for both systems, GaSb/Si interfaces exhibit imperfect arrays of misfit dislocations and possible chemical intermixing, while AlSb/Si interfaces are significantly more abrupt, with a much more regular array of 90° misfit dislocations.[5,6]

In this work, we provide a qualitative and quantitative analysis of III-Sb islands on (001) silicon in the frame of the Wulff-Kaishew (WK) theorem[8–10] also known as Winterbottom theory,[11] which predicts the equilibrium island shape in the VW growth mode from surface and interface energies. Conversely, information on surface and interface energies can be deduced from experimental shapes. This was applied to oxides, metallic, or more scarcely to semiconductor systems.[12–14] Here, we first analyze AlSb islands grown on vicinal Si and covered by thick GaSb layers. We then apply the procedure to previous results presented in the literature.[4–6] General tendencies on the interface energies are established, which explain the different shapes of GaSb and AlSb islands.

AlSb deposits of 0, 4, 17, 30, and 50 MLs were grown at 450 °C by MBE on (001)Si with an offcut of 6° towards the [110] direction. Thick GaSb layers were then grown at 500 °C. More growth details were provided elsewhere.[7] The samples were thinned by FIB and examined by scanning transmission electron microscopy (STEM).

Figure 1 displays STEM observations along the silicon ⟨110⟩ direction parallel to the steps of various samples. In the absence of AlSb, numerous voids (generally {111} facetted) are formed at the GaSb/Si interface [Fig. 1(a)]. In contrast, AlSb islands formed with 4 to 50 ML deposits had consistently a trapezoidal profile [Figs. 1(b)–1(d)]. The (001) top facet and lateral {111} facets were identified in energy-dispersive x-ray (EDX) cartographies or atomic resolved STEM images [Figs. 1(b)–1(d)]. Higher index facets were not detected. Extended defects and antiphase domains are discussed elsewhere.[7,15]

Before analyzing these island shapes, we recall that the wetting factor is[10]

$$\Phi = \gamma_{(001)} + \gamma_i - \gamma_{Si}, \tag{1}$$

where $\gamma_{(001)}$ and γ_{Si} are the (001) surface energies of the deposit and the Si substrate, respectively, and γ_i the interface energy. The growth is 2D if Φ is negative (complete wetting), 3D VW if Φ is positive (partial wetting), and there is no more adhesion above $2\gamma_{(001)}$.[8] Applying the Wulff

a)Author to whom correspondence should be addressed: anne.ponchet@cemes.fr

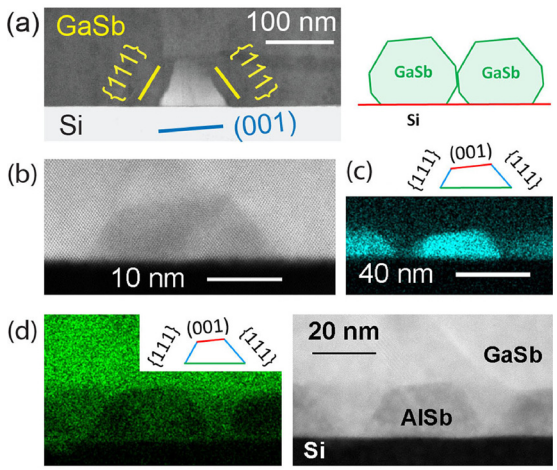

FIG. 1. STEM observations along the ⟨110⟩ direction parallel to the steps of the vicinal Si substrate. (a) GaSb grown on bare Si with a typical {111} facetted void attributed to the coalescence of two GaSb islands. (b) Atomically resolved image of 4 ML AlSb. (c) Aluminum EDX mapping of 30 ML AlSb. (d) Gallium EDX mapping and STEM image of 50 ML AlSb.

construction to the deposit, the equilibrium shape of the free crystal is established from the so-called Wulff point (WP). Then, the WK construction consists in positioning the interface such that

$$\frac{h_{hkl}}{\gamma_{(hkl)}} = \frac{h_i}{\gamma_i - \gamma_{Si}}, \tag{2}$$

where h_i is the distance to the WP of the interface, and h_{hkl} is the distance to the WP of any {hkl} stable facet of the free crystal with a γ_{hkl} surface energy.[9,10] By construction, h_i is positive (negative) if $(\gamma_i - \gamma_{Si})$ is positive (negative), and the interface is then below (above) the WP [Fig. 2(a)].

The predicted island shape is size independent in the absence of elastic effects.[10] A trapezoidal profile of width b and height h [Fig. 2(b)] is thus characterized by an aspect ratio $k = h/b$. The angle between {111} and (001) is $\alpha = 54.7°$. Given the construction in Fig. 2(c), where the isosceles triangle has a base $b_0 = 2h_{111}/\sin\propto$ and a height $h_0 = h_{111}/\cos\propto$, it becomes

$$b = b_0\frac{h_0 + h_i}{h_0} = \frac{2}{\tan\propto}\left(\frac{h_{111}}{\cos\alpha} + h_i\right).$$

Actually, with the ⟨111⟩ directions (III–V bond directions) being polar, {111}A and {111}B surfaces differ and have not the same energy. Each III–V island has thus two widths b_A and b_B. As $h = h_{001} + h_i$, two aspect ratios k_A and k_B are predicted applying (2)

$$k_A = \frac{h}{b_A} = \frac{\tan\propto\,(\gamma_{(001)} + \gamma_i - \gamma_{Si})}{2\left(\frac{\gamma_{(111)A}}{\cos\,\alpha} + \gamma_i - \gamma_{Si}\right)}, \tag{3a}$$

$$k_B = \frac{h}{b_B} = \frac{\tan\propto\,(\gamma_{(001)} + \gamma_i - \gamma_{Si})}{2\left(\frac{\gamma_{(111)B}}{\cos\,\alpha} + \gamma_i - \gamma_{Si}\right)}. \tag{3b}$$

Now, one can reverse the construction to get relations between surface and interface energies from the experimental aspect ratios. By rewriting (3a) and (3b), it becomes

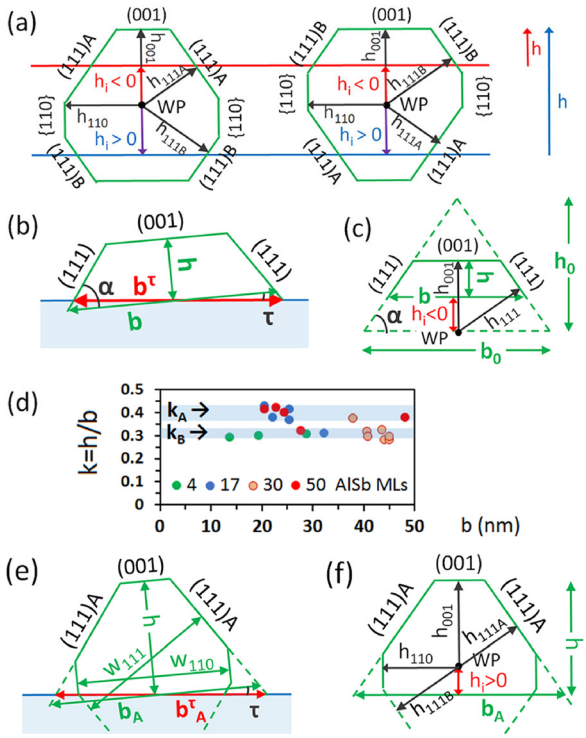

FIG. 2. (a) {110} projections of the WK construction applying Eq. (2) to a cubic III–V grown on (001)Si with stable facets {001}, {110}, and {111}A and B. The interface is below (blue line) or above (red line) the WP if $h_i > 0$ or <0, respectively. (b) Scheme of a trapezoidal experimental profile of height h and base b (for a vicinal substrate, the apparent base is b^τ and as the tilt τ is small, a first order development in τ gets $b = b^\tau$) and (c) correspondence with h_{001}, h_{111}, and h_i. (d) Experimental $k = h/b$ of AlSb islands (this work) as a function of b; the blue bands suggest the double distribution k_A, k_B. (e) Scheme of an experimental profile with emerging vertical {110} facets as GaSb islands in Ref. 6 and (f) correspondence with h_{001}, h_{111A}, h_{111B}, h_{110}, and h_i.

$$\frac{\gamma_{(111)B}}{\gamma_{(001)}} = \frac{(\tan\propto\,-2\,k_B)\,k_A\frac{\gamma_{(111)A}}{\gamma_{(001)}} + \sin\propto\,(k_B - k_A)}{(\tan\propto\,-2\,k_A)\,k_B}, \tag{4}$$

$$\frac{\gamma_i - \gamma_{Si}}{\gamma_{(001)}} = \frac{2\,k_A\frac{\gamma_{(111)A}}{\gamma_{(001)}} - \sin\propto}{\sin\propto\,-2\,k_A\cos\propto}. \tag{5}$$

Due to the different crystal structures of III–Vs and Si, the islands grow on (001) Si with two polarity variants. Two different profiles characterized by k_A and k_B, respectively, could be observed simultaneously in the same {110} plane. In the following, as we cannot determine which observed {111} facets have the A or B orientation, we will arbitrarily note A those with the largest relative extension (*i.e.*, we assume that $\gamma_{(111)A} < \gamma_{(111)B}$). If neither of the profiles displays vertical (110) or (1 $\bar{1}$ 0) facets, we deduce that 2 h_{110} is always larger than b. As $k_A > k_B$, $\gamma_{(110)}/\gamma_{(001)}$ is thus larger than

$$\left(\frac{\gamma_{(110)}}{\gamma_{(001)}}\right)_{min} = \left(1 + \frac{\gamma_i - \gamma_{Si}}{\gamma_{(001)}}\right)\frac{1}{2\,k_B}. \tag{6}$$

Equations (4), (5), and (6) constitute the reverse WK construction solutions for experimental trapezoidal profiles. As the solution is not unique, the exact position of the WP

remains experimentally unknown. Here, we chose to express all possible solutions in the form $\gamma_{(111)B}/\gamma_{(001)}$, $(\gamma_i - \gamma_{Si})/\gamma_{(001)}$ and $(\gamma_{(110)}/\gamma_{(001)})_{min}$ as a function of $\gamma_{(111)A}/\gamma_{(001)}$. Boundaries guaranty the simultaneous stability of low index facets ($\beta = 45°$)

$$\cos\propto < \frac{\gamma_{(111)A}}{\gamma_{(001)}} < \frac{\gamma_{(111)B}}{\gamma_{(001)}} < \frac{1}{\sin\propto}$$

and

$$\cos\beta < \frac{\gamma_{(110)}}{\gamma_{(001)}} < \frac{1}{\sin\beta}.$$

As a first and direct conclusion, the {111} facetted voids at the GaSb/Si interface [Fig. 1(a)] are attributed to the coalescence of large islands with the interface below the WP [Fig. 2(a)]. On the contrary, the AlSb/Si interface was above. Without hypothesis on the surface energies, this demonstrates that $(\gamma_i - \gamma_{Si})$ is negative (positive) for AlSb/Si (GaSb/Si).

Experimental aspect ratios are displayed as a function of the AlSb island size b [Fig. 2(d)]. We eliminated coalesced islands and polycrystalline islands not suitable for the WK analysis. We considered nevertheless islands with isolated stacking faults or micro-twins not affecting the faceting. The WK description supposes that the equilibrium shape is achieved. The growth shape can differ from the equilibrium shape. However, even though MBE is considered as a non-equilibrium technique, some growth conditions and materials systems favor the spontaneous evolution of the deposit towards the near-equilibrium stage.[16] The size independence of the shape is known as a criterion for describing the islands with the WK construction. All islands are plastically relaxed due to the 14% misfit (the critical thickness is around 1 monolayer). The effect of residual elastic strain on the island shape[10] can thus be neglected. Here, the aspect ratios are restricted to the 0.28–0.43 interval and a double distribution centered on $k_A = 0.40$ (standard deviation SD $\approx$ 0.03) and $k_B = 0.31$ (SD $\approx$ 0.02) can be proposed [Fig. 2(d)]. This is in agreement with the observation in all samples of the anti-phase domains that originated from AlSb islands of the two polarity variants (also reported in Ref. 15). For instance, in Figs. 1(b) and 1(c), the aspect ratios were 0.31 and 0.28 for b = 28 nm and 45 nm, respectively, and are attributed to the profile with B facets. In Fig. 1(d), k = 0.38 and is attributed to the profile with A facets. So, while b globally increased with the deposited amount, given the error bar (≈10%) the aspect ratios could be considered as independent of the island size. The shape is also independent of the AlSb amount (from 4 to 50 MLs), which reinforces the hypothesis of close-to-equilibrium shapes. On this basis, the solutions of the reverse WK construction are displayed in Fig. 3 (blue curves).

To validate our approach, we also considered different III-Sb islands previously reported. Large GaSb islands grown by Kim *et al.* on nominal Si are particularly suitable for a precise experimental analysis. Except a few polycrystalline box-shaped islands, TEM ⟨110⟩ cross-sectional observations revealed trapezoidal profiles with sharp {111} facets [Fig. 2(a) in Ref. 5]. We found 2 aspect ratios: 0.44 ± 0.01 for 2 islands and 0.35 ± 0.02 for 5 islands, which we attributed to the two GaSb variants. The energy ratios are then deduced (red dashed curves Fig. 3). GaSb islands formed on a thin AlSb template were significantly flatter [Fig. 2(b) of Ref. 5]. We approximately measured 0.24 and 0.18 as k_A and k_B with a larger dispersion of about 10% due to partial coalescence. The corresponding energy ratios are displayed in red continuous lines.

Micrometric GaSb islands grown on vicinal Si by Vajargah *et al.* exhibited in addition vertical {110} facets while {111}A and B facets can be simultaneously seen by TEM [Fig. 1(a) of Ref. 6]. Most islands have coalesced producing {111} facetted interfacial voids. We deduced that the interface was significantly below the WP. The dimensions of an island profile with A facets [Figs. 2(e) and 2(f)] are h, b_A, $w_{110} = 2h_{110}$, and the distance between two opposite {111} facets $w_{111} = h_{111A} + h_{111B}$. There are 3 aspect ratios $k_A = h/b_A$, $k_{110} = h/w_{110}$, and $k_{A+B} = h/w_{111}$. The solutions as a function of $\gamma_{\{111\}A}/\gamma_{(001)}$ are now Eqs. (5), (7), and (8)

$$\frac{\gamma_{(110)}}{\gamma_{(001)}} = \left(1 + \frac{\gamma_i - \gamma_{Si}}{\gamma_{(001)}}\right)\frac{1}{2\,k_{110}}, \tag{7}$$

$$\frac{\gamma_{(111)B}}{\gamma_{(001)}} = -\frac{\gamma_{(111)A}}{\gamma_{(001)}} + \left(1 + \frac{\gamma_i - \gamma_{Si}}{\gamma_{(001)}}\right)\frac{1}{k_{A+B}}. \tag{8}$$

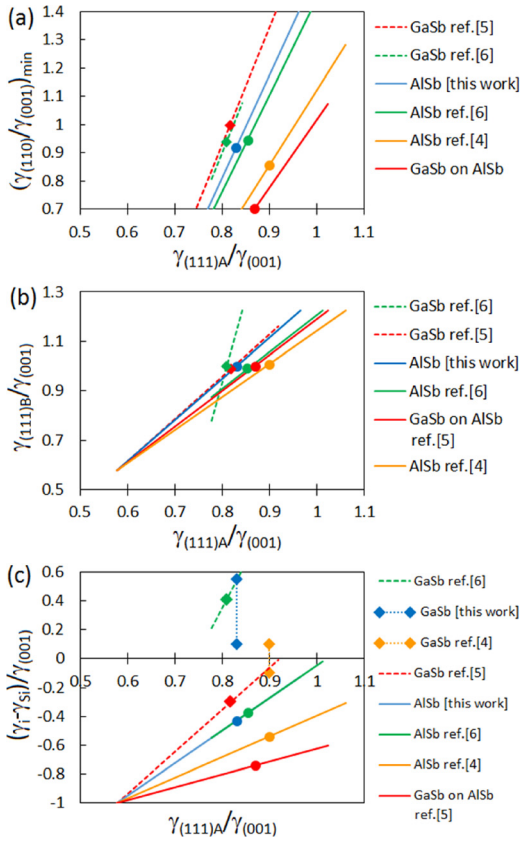

FIG. 3. Solutions of the reverse WK construction as a function of $\gamma_{\{111\}A}/\gamma_{(001)}$. (a) Equation (6) $(\gamma_{(110)}/\gamma_{(001)})_{min}$ for this work and Refs. 4 and 5 or Eq. (7) $\gamma_{(110)}/\gamma_{(001)}$ for GaSb of Ref. 6. (b) Equation (4) $\gamma_{(111)B}/\gamma_{(001)}$ for this work and Refs. 4 and 5 or Eq. (8) $(\gamma_{(111)B}/\gamma_{(001)})_{min}$ for GaSb of Ref. 6. (c) Equation (5) $(\gamma_i - \gamma_{Si})/\gamma_{(001)}$ for this work and Refs. 4–6. The vertical dotted lines suggest possible values for GaSb/Si interfaces of this work and Ref. 4. For each case, the particular solution minimizing the differences between $\gamma_{(111)A}$, $\gamma_{(111)B}$, and $\gamma_{(001)}$ is highlighted by a square (GaSb) or a circle (AlSb and [GaSb on AlSb]).

Due to coalescence, a statistical analysis was not possible and only one isolated island could have been analyzed ($k_A = 0.55$, $k_{110} = 0.75$, and $k_{A+B} \leq 0.78$). The solutions are displayed in Fig. 3 by green dashed lines [for Fig. 3(b): $(\gamma_{\{111\}B}/\gamma_{(001)})_{min}$ using $k_{A+B} = 0.78$]. AlSb islands had trapezoidal profiles with a height of 20 nm and width around 50 to 60 nm.[6] We thus estimated energy ratios (green continuous lines) using $k_A = 0.40$ and $k_B = 0.33$ for AlSb/Si.

In the precursor study by Akahane *et al.*[4] (yellow lines in Fig. 3), GaSb islands had a quasi-rounded in-plane shape with h over width ≈0.5, suggesting that the interface was close to the WP. AlSb islands were elongated. We found $k_A = 0.32 \pm 0.01$ and $k_B = 0.27 \pm 0.01$ from the average heights and widths reported in Fig. 3 of Ref. 4 (the error bar does not reflect the dispersion from one island to another). k_A and k_B are similar for 3 and 5 nm AlSb deposits, while the average h was 14 nm and 18 nm, respectively.

We first discuss the surface energy ratios generated by these reverse WK constructions [Figs. 3(a) and 3(b)]. They are rather similar for the different sets of experimental islands. It is likely that the stable facets of the crystal do not have too different energies.[17,18] The particular solutions minimizing the differences between $\gamma_{(111)A}$, $\gamma_{(111)B}$, and $\gamma_{(001)}$ are thus highlighted by squares (GaSb) or circles (AlSb). For instance, for the particular solution for GaSb islands of Ref. 5, $(\gamma_{(001)} - \gamma_{(111)A})/\gamma_{(001)} = 0.18$, $(\gamma_{(001)} - \gamma_{(111)B})/\gamma_{(001)} = 0.02$, and $(\gamma_{(111)B} - \gamma_{(111)A})/\gamma_{(001)} = 0.16$ and any other solution leads to one of these differences larger than 0.18. These solutions (also reported in Table I) are very close from each other. The actual physical solutions should be close to them. These highlighted ratios are also close to their counterparts calculated by density functional theory (DFT) in GaAs and InAs (between 0.85 and 1.1 for the As-rich range of the chemical potential variation).[17,18]

DFT calculated energies of the cleaved stoichiometric {110} surfaces are 42.6 and 46.5 meV/A^2 for GaSb and AlSb, respectively.[19] They are proportional to the cohesion energy and can be used as common references. Absolute data for other III-Sb surfaces are lacking. By analogy with III-As[17,18] and from DFT study of III-Sb (001) reconstructions,[20] we nevertheless can assume that, when switching from GaSb to AlSb, $\gamma_{(hkl)}$ increases by the same order of magnitude as $\gamma_{(110)}$ (9%[19]).

Coming back to (1), we can now discuss the role of the interface energy. The better wetting of Si by AlSb than by GaSb that is consistently observed cannot be explained by the difference in $\gamma_{(001)}$ (that would slightly favor the reverse behavior). Interfaces have clearly a major impact [Fig. 3(c)]: for each study, $(\gamma_i - \gamma_{Si})/\gamma_{(001)}$ is larger for GaSb/Si than for AlSb/Si (including hereafter [GaSb on AlSb]/Si). The difference for the particular solutions for this work, Refs. 5, 6, and 4, is >0.43, 0.43, 0.79, and ≈0.54, respectively (from Table I). This difference is really significant, given that $(\gamma_i - \gamma_{Si})/\gamma_{(001)}$ lies between −1 and +1 in the VW growth mode. It is thus entirely responsible for the larger wetting by AlSb than by GaSb.

The accuracy of each solution is only limited by the accuracy in aspect ratios. For instance, for AlSb islands of our work, $k_A = 0.40 \pm 0.03$ gives $(\gamma_i - \gamma_{Si})/\gamma_{(001} = -0.43 \pm 0.09$ for the solution $\gamma_{(111)A}/\gamma_{(001)} = 0.83$. The difference in $(\gamma_i - \gamma_{Si})/\gamma_{(001)}$ when switching from GaSb/Si to AlSb/Si depends in addition on the chosen solution. However, our estimate would not drastically change with moderate variations around the solutions reported in Table I. A 5% increase in $\gamma_{(111)A}/\gamma_{(001)}$ induces a 22% increase in $(\gamma_i - \gamma_{Si})/\gamma_{(001)}$. The accuracy is considerably improved with decreasing k_A [from Eq. (5)].

TABLE I. Particular solutions of the reverse WK constructions that minimize the differences between the III-Sb surface energies $\gamma_{(111)A}$, $\gamma_{(111)B}$, and $\gamma_{(001)}$.

Analyzed islands	$\gamma_{(111)A}/\gamma_{(001)}$	$\gamma_{(111)B}/\gamma_{(001)}$	$\gamma_i - \gamma_{Si}/\gamma_{(001)}$
GaSb (this work)			>0
AlSb (this work)	0.83	1.00	−0.43
GaSb in Ref. 5	0.82	0.98	−0.31
GaSb on AlSb in Ref. 5	0.87	1.01	−0.74
GaSb in Ref. 6	0.81	1.00	0.41
AlSb in Ref. 6	0.85	0.99	−0.38
GaSb in Ref. 4			≈0
AlSb in Ref. 4	0.90	1.01	−0.54

Absolute orders of magnitude can also be estimated, assuming from Fig. 3(a) that $\gamma_{(110)}/\gamma_{(001)} \approx 0.9$ to 1

$$(\gamma_i - \gamma_{Si})^{GaSb/Si} - (\gamma_i - \gamma_{Si})^{AlSb/Si} > 21, \approx 22, \approx 38, \approx 27 \text{ in meV/A}^2 \quad (9)$$

for this work, Refs. 5, 6, and 4, respectively. Interface energies are macroscopic resultants of several microscopic contributions: chemical discontinuity (III-Si and/or Sb-Si bonds), misfit dislocation array, other defects, and chemical intermixing. On the theoretical basis of $\gamma_{Si} = 90$ meV/A^2,[3,21] γ_i is in the range of 55–70 meV/A^2 for AlSb/Si and 75–110 meV/A^2 for GaSb/Si. As a comparison, the calculated energy of a perfect GaP/Si interface (pure chemical discontinuity) was around 30–45 meV/A^2,[3] while from the Matthews model,[10] the energy of a perfect 90° misfit dislocation array is about 50–60 meV/A^2 for AlSb and GaSb on Si. Thus, 55–70 meV/A^2 appears as rather coherent with the microscopic observations of abrupt and regular AlSb/Si interfaces.[5,6] The extra 20–40 meV/A^2 for GaSb/Si interfaces in (9) is thus probably correlated with their numerous structural imperfections. These estimations of absolute interface energies are based on DFT calculations for perfect surfaces at 0 K, which may differ from actual surface structures and growth conditions. In particular, γ_{Si} can vary with the surface preparation process and can eventually be modified by adsorption of residual III or V elements.

Finally, all reported differences in shape[4–6] between GaSb islands (high with a quasi-rounded in-plane shape), and AlSb islands (flat and elongated), can be fully explained without resorting to any kinetics mechanism. Indeed, for a weak wetting ($\gamma_i - \gamma_{Si} > 0$), the top-view shape is inscribed in an octagon defined by vertical {100} and {110} facets [Fig. 4(a)], as is the free crystal. For a larger wetting ($\gamma_i - \gamma_{Si} < 0$), only the (001) top facet and inclined {111} and {101} facets subsist [Figs. 4(b) and 4(c)]. As soon as $\gamma_{\{111\}B}$ differs from $\gamma_{\{111\}A}$ (ratio 1.20 here), the top-view shape is elongated. Obviously, the more these energies are different the more elongated the shape is. More interestingly, for a

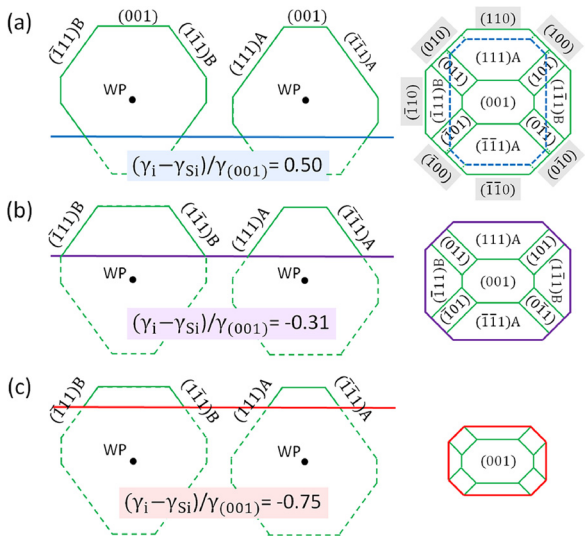

FIG. 4. [110] profile, [1-10] profile, and top-view of the WK construction with various interfacial energies and $\gamma_{\{111\}A}/\gamma_{(001)} = 0.82$, $\gamma_{\{111\}B}/\gamma_{(001)} = 0.98$, and $\gamma_{\{110\}}/\gamma_{(001)} = 0.99$ (highlighted values from analysis of GaSb islands of Ref. 5). (a) If $(\gamma_i - \gamma_{Si})/\gamma_{(001)} > 0$, the island top-view shape is inscribed in an octagon as the free crystal (the dashed blue line indicates the interface, below the WP. Facets with a grey background are vertical in top-view). (b) If $(\gamma_i - \gamma_{Si})/\gamma_{(001)} < 0$, the top-view shape is elongated. (c) With a lower $(\gamma_i - \gamma_{Si})/\gamma_{(001)}$ (i.e., a larger adhesion), the island base is even more elongated.

given Wulff shape, the larger the adhesion is the flatter the island is and also the more it is elongated in top view, as seen in Figs. 4(b) and 4(c). The in-plane aspect ratio w_B/w_A of the top (001) facet (w_A and w_B being its widths along $\langle 110 \rangle$) is an intrinsic property of the III–V, while the in-plane aspect ratio at the island base, b_B/b_A, depends also on $(\gamma_i - \gamma_{Si})$ [from Eq. (3)]

$$\frac{w_B}{w_A} = \frac{k_A(\tan \propto - 2k_B)}{k_B(\tan \propto - 2k_A)} = \frac{\gamma_{(111)B} - \cos \propto \gamma_{(001)}}{\gamma_{(111)A} - \cos \propto \gamma_{(001)}}, \quad (10a)$$

$$\frac{b_B}{b_A} = \frac{k_A}{k_B} = \frac{\gamma_{(111)B} + \cos \propto (\gamma_i - \gamma_{Si})}{\gamma_{(111)A} + \cos \propto (\gamma_i - \gamma_{Si})}. \quad (10b)$$

For the GaSb islands of Ref. 5, from the cross-sectional double distribution $k_A = 0.44 \pm 0.01$ and $k_B = 0.35 \pm 0.02$, we predict $b_B/b_A = 1.26 \pm 0.1$ and $w_B/w_A = 1.7 \pm 0.3$. This predicted top-view shape [Fig. 4(b)] agrees with experimental top-view observations [Fig. 1(b) of Ref. 5] showing faceted GaSb islands of the two variants with in-plane aspect ratios of about 1.1 (base) and 1.6 (top).

To conclude, thanks to the reverse WK construction, ratios of energies of all low index surfaces were experimentally estimated for the III-Sb of this work and other studies.[4–6] Given the theoretical surface energies of III-Sb and Silicon (about 45 and 90 meV/A^2, respectively), the VW growth mode of III-Sb on Si is unambiguously attributed to the high interface energy γ_i (55 to 110 meV/A^2). The larger wetting by AlSb than by GaSb, which is consistently observed, can now be clearly attributed to a significant difference in γ_i. The increase in $(\gamma_i - \gamma_{Si})/\gamma_{\{001\}}$ when switching from AlSb to GaSb is in the range of 0.4–0.8, depending on the study, and the increase in γ_i is around 20 to 40 meV/A^2. This difference reflects macroscopically the larger interface disorder in GaSb/Si than in AlSb/Si already reported at the microscopic level.[5,6] Our analysis also contributes to explain why the AlSb/Si template, by decreasing the interface energy, systematically improves the subsequent growth of GaSb.

All experimental shapes are qualitatively and quantitatively explained by the theory of wetting in crystals, as expected for equilibrium shapes in a pure VW growth mode. Finally, the degree of the in-plane island elongation is directly related to its degree of adhesion, *i.e.*, to the interfacial properties. This relation is due to the polar character of {111} directions and can be generalized to any cubic compound semiconductor (III–V, II–VI) growing in the VW mode.

This work was supported by the French National Research Agency ANTIPODE Project (Grant No. ANR-14-CE26-0014). The authors gratefully acknowledge M. J. Casanove for critical reading of the manuscript.

[1]E. Tournié, J. B. Rodriguez, L. Cerutti, H. Y. Liu, J. Wu, and S. M. Chen, MRS Bull. **41**(3), 218 (2016).
[2]M. Borg, H. Schmid, K. E. Moselund, G. Signorello, L. Gignac, J. Bruley, C. Breslin, P. Das Kanungo, P. Werner, and H. Riel, Nano Lett. **14**, 1914 (2014).
[3]See, I. Lucci, S. Charbonnier, L. Pedesseau, M. Vallet, L. Cerutti, J.-B. Rodriguez, E. Tournié, R. Bernard, A. Létoublon, N. Bertru, A. Le Corre, S. Rennesson, F. Semond, G. Patriarche, L. Largeau, P. Turban, A. Ponchet, and C. Cornet, Phys. Rev. Mater. **2**, 060401(R) (2018); References therein.
[4]K. Akahane, N. Yamamoto, S. Gozu, A. Ueta, and N. Ohtani, J. Cryst. Growth **283**, 297 (2005).
[5]Y. H. Kim, Y. K. Noh, M. D. Kim, J. E. Oh, and K. S. Chung, Thin Solid Films **518**, 2280 (2010).
[6]S. H. Vajargah, S. Ghanad-Tavakoli, J. S. Preston, R. N. Kleiman, and G. A. Botton, J. Appl. Phys. **114**, 113101 (2013).
[7]J. B. Rodriguez, L. Cerutti, G. Patriarche, L. Largeau, K. Madiomanana, and E. Tournié, J. Cryst. Growth **477**, 65 (2017).
[8]M. Wolmer and A. Weber, Z. Phys. Chem. **119**, 277 (1926).
[9]R. Kaishew, Arbeitstatung Festkörper Phys., Dresden **1952**, 81; Commun. Bulg. Acad. Sci. **1**, 100 (1950).
[10]P. Müller and R. Kern, Surf. Sci. **457**, 229 (2000).
[11]W. Winterbottom, Acta Metall. **15**, 303 (1967).
[12]C. R. Henry, Prog. Surf. Sci. **80**, 92 (2005).
[13]S. Stankic, R. Cortes-Huerto, N. Crivat, D. Demaille, J. Goniakowski, and J. Jupille, Nanoscale **5**, 2448 (2013).
[14]M. D. Korzec, M. Roczen, M. Schade, B. Wagner, and B. Rech, J. Appl. Phys. **115**, 074304 (2014).
[15]M. Niehle, J.-B. Rodriguez, L. Cerutti, E. Tournié, and A. Trampert, Acta Mater. **143**, 121 (2018).
[16]J. Tersoff, M. D. Johnson, and B. G. Orr, Phys. Rev. Lett. **78**, 282 (1997).
[17]N. Moll, A. Kley, E. Pehlke, and M. Scheffler, Phys. Rev. B **54**, 8844 (1996).
[18]E. Pehlke, N. Moll, A. Kley, and M. Scheffler, Appl. Phys. A **65**, 525 (1997).
[19]W. Liu, W. T. Zheng, and Q. Jiang, Phys. Rev. B **75**, 235322 (2007).
[20]J. Houze, S. H. Kim, S.-G. Kim, S. C. Erwin, and L. J. Whitman, Phys. Rev. **B76**, 205303 (2007).
[21]G.-H. Lu, M. Huang, M. Cuma, and F. Liu, Surf. Sci. **588**, 61 (2005).